Cement and Concrete Research 175 (2024) 107371

Contents lists available at ScienceDirect

Cement and Concrete Research

journal homepage: www.elsevier.com/locate/cemconres

Stacking faults of the hydrous carbonate-containing brucite (HCB) phase in hydrated magnesium carbonate cements

Daniel Jansen [a,**], Alexander German [b,c], Dominique Ectors [a], Frank Winnefeld [b,*]

[a] Friedrich-Alexander-Universität Erlangen-Nürnberg, GeoZentrum Nordbayern, Mineralogy, Schlossgarten 5a, 91054 Erlangen, Germany
[b] Empa, Swiss Federal Laboratories for Materials Science and Technology, 8600 Dübendorf, Switzerland
[c] ETH Zürich, Institute for Building Materials, 8093 Zürich, Switzerland

ARTICLE INFO

Keywords:
Magnesium carbonate cements
Low-CO_2 binders
Brucite
Hydromagnesite
Mineral carbonation

ABSTRACT

Recently, a hydrous carbonate-containing brucite (HCB) with an approximate composition of $MgCO_3$·35 Mg$(OH)_2$·H_2O was postulated as hydration product of binders based on mixtures of reactive magnesia and hydromagnesite ($Mg_5(CO_3)_4(OH)_2·4H_2O$). X-ray diffraction showed that the 001 reflection of this phase was split into two reflections at 20 °C, whereas at 60 °C only one reflection occurred. Rietveld refinement revealed that the X-ray pattern of the HCB-phase could be fitted well when a random displacement (stacking faults) and a movement of the layers in x, y and z direction were allowed. The presence of water and/or carbonate leads to different distances between the layers, thus causing the splitting of the 001 reflection. At 60 °C, only carbonate is included in the brucite structure, leading to a similar distance between all brucite layers. The assignment of the additional reflection appearing at 20 °C to a separate, unknown hydrated magnesium carbonate, as suggested in earlier studies, can be excluded.

1. Introduction

Binders based on magnesium oxide derived from magnesium silicates (so-called "MOMS") or other Mg sources such as rejected brines have been proposed as a potential low-CO_2 or even carbon negative cementitious binder [1,2]. One type of these binders are blends of reactive magnesia with hydrated magnesium carbonates (HMCs) such as hydromagnesite, $Mg_5(CO_3)_4(OH)_2·4H_2O$, which had been developed and patented within the framework of the "Novacem" start-up venture [3–5]. Mortars with reactive magnesia as sole binder component do not develop significant compressive strengths, while in blends with HMCs a compressive strength comparable to the one of mortars based on Portland cement can be achieved [6]. Two more recent studies focussed more in detail on the hydrate assemblage of MgO/hydromagnesite binders [7,8]. The brucite ($Mg(OH)_2$) formed in such binders shows broad and partially shifted reflections in its X-ray diffraction pattern, and the authors concluded that strength formation must be related to this kind of brucite. Based on current thermodynamic data [9,10], artinite, $Mg_2(CO_3)(OH)_2·3H_2O$, was predicted as thermodynamic stable phase, but could not be identified. The reason might be either a slow kinetics of formation or uncertainties of the thermodynamic data of artinite available in literature. In [7,8] it is suggested based on X-ray diffraction, thermogravimetry and vibrational spectroscopy that besides the poorly crystalline brucite an additional HMC phase of unknown composition may be present. However, it remained still unclear whether two separate phases, a poorly crystalline brucite and an unknown HMC, are present, or if only a brucite-like phase occurs, which additionally contains carbonate and water. In our recent work [11,12], we came to the conclusion that the latter is the case and postulated the presence of a hydrous carbonate-containing brucite (HCB) as sole hydration product of MgO/hydromagnesite binders. The additional intake of carbonate and water into the structure of brucite should then be the reason for the shift of the reflections in the X-ray diffraction patterns and the appearance of an additional reflection, which was previously assigned to an unknown HMC. It was concluded that the alteration of the brucite structure might be related to stacking faults. This hypothesis is tested in the present study by means of X-ray diffraction combined with Rietveld refinements. Notably similar observations of a peak splitting due to stacking faults / interstratification on $Ni(OH)_2$, which is isostructural to brucite, have been made [13].

* Corresponding author at: Empa, Swiss Federal Laboratories for Materials Science and Technology, Laboratory for Concrete and Asphalt, Überlandstrasse 129, 8600 Dübendorf, Switzerland.
** Correspondence to: Friedrich-Alexander-Universität Erlangen-Nürnberg, GeoZentrum Nordbayern, Mineralogy, Schlossgarten 5a, 91054 Erlangen, Germany.
E-mail addresses: daniel.jansen@fau.de (D. Jansen), frank.winnefeld@empa.ch (F. Winnefeld).

https://doi.org/10.1016/j.cemconres.2023.107371
Received 11 July 2023; Received in revised form 19 October 2023; Accepted 2 November 2023
Available online 17 November 2023

In literature it has been described that minerals having a layered structure (such as clay minerals or brucite) might show a random displacement (stacking faults) [14] and/or a rotation of layers (also known as turbostratic disorder) [15] resulting in complex X-ray diffraction patterns. This has found recent interest in the construction industry as important minerals which are used as sources of supplementary cementitious materials such as kaolinite might show stacking faults. The approach is based on the concept that single layers of layered structures can be displaced against each other in the respective crystallographic directions. In order to implement the approach, a basic layer has to be described which is then stacked up to a certain amount of stacks. The stacks are allowed to move against each other (see Fig. 1).

This approach can be used for the Rietveld refinement of layered structures such as kaolinite [16,17], resulting in significant improvement of phase quantification, see Fig. S1 in the Electronic Supplementary Material (ESM). Similar models have also been used successfully to quantify different smectite clay minerals [18,19].

The present study aims to verify by Rietveld refinements of XRD patterns of hydrated MgO/hydromagnesite blends, if (i) a poorly crystalline brucite-like phase is the only hydrate phase or if an unknown HMC is present as additional hydrate phase, and if (ii) the broad and shifted reflections of the brucite-like phase can be explained by stacking faults.

2. Materials

A blend of 70 mass-% MgO and 30 mass-% hydromagnesite was prepared using reactive MgO and laboratory-grade hydromagnesite (Alfa Aesar, Germany). Reactive MgO was synthesized by firing laboratory-grade brucite (Fisher Scientific, UK) in a lab furnace at 900 °C for 6 h. Chemical composition and phase purity of brucite, MgO and hydromagnesite were characterized with X-ray fluorescence (XRF), X-ray diffraction (XRD), and thermogravimetry (TGA) within another study (see [11] for further details). Additionally, bulk density and specific surface area were examined and are provided in [11] as well.

Pastes were obtained by mixing 10 g of unhydrated binder with 12 g of deionized water with spatula by hand. The samples were cured in plastic vessels at 20 and 60 °C for 12 months.

Afterwards, the hydration of the pastes was stopped by organic solvent exchange using isopropanol and diethyl ether adapted after [21]. The obtained solid was ground to a particle size below 63 µm using an agate pestle and mortar and used for further analyses.

3. Methods

3.1. Previous investigations of the samples

The two pastes were characterized by thermogravimetric analysis (TGA) coupled with Fourier transform infrared (FTIR) spectroscopy and solid state ^{13}C cross-polarization magic angle spinning nuclear magnetic resonance spectroscopy (^{13}C CP-MAS NMR).

TGA-FTIR measurements were performed with a TGA instrument STA 449 F3 Jupiter (Netzsch, Germany) to an IR Alpha detector (Bruker AG, Germany) for gas analysis from 30 to 1000 °C with a heating rate of 10 K/min under N_2 atmosphere. Absorbance data from FTIR was integrated at a wavenumber range of 1300–2000 cm^{-1} and 2200–2400 cm^{-1} to calculate IR signals of H_2O and CO_2 respectively. The amount of unreacted HY was calculated according to Eq. (1).

$$m\,(HY)_{hyd.} = \frac{mass\ loss\ of\ HY\ (500-550°C)_{hyd.}}{mass\ loss\ of\ HY\ (500-550°C)_{reference}} \quad (1)$$

^{13}C CP-MAS NMR measurements were conducted using a Bruker Advance III 400 NMR spectrometer (Bruker BioSpin AG, Switzerland). NMR spectra were recorded at 100.6 MHz, using a 7 mm CP-MAS NMR probe at 4000 Hz MAS rotation rates. Obtained NMR data was treated with "DMFIT" software [22] to determine relative signal intensities of observed resonances applying Lorentzian shapes. The amount of unreacted hydromagnesite in the hydrated samples was calculated according to [11] involving normalizing of signal intensities of hydromagnesite resonances by the weight and by the number of scans with respect to a hydromagnesite reference.

The reader is referred to [11] for further information on the methods.

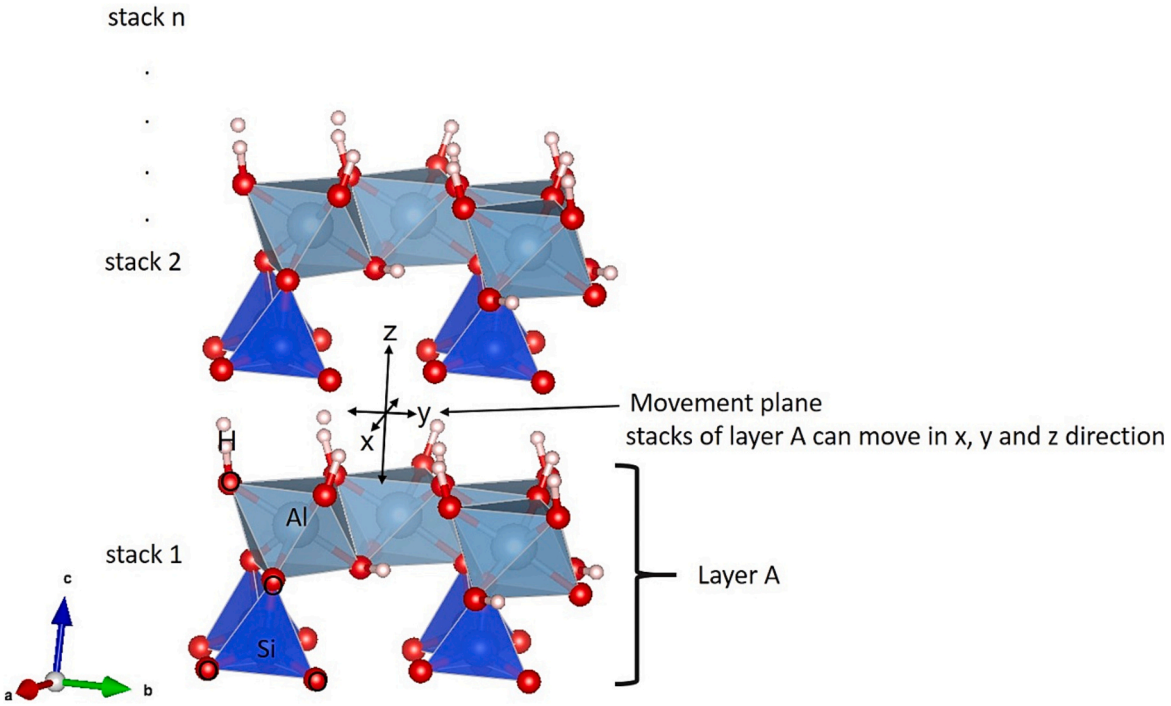

Fig. 1. Visualization of stacking layers in the kaolinite structure as well as movement plane and moving directions for stacking faults between repeating layer A (Visualization done using VESTA 3 [20]).

3.2. Rietveld analysis and stacking faults modelling

To obtain the X-ray diffraction (XRD) patterns for Rietveld analysis, the samples were prepared into front loading sample holders. Measurements were performed using a Bruker D8 diffractometer in Bragg-Brentano geometry with an angular range from 4 to 80° 2θ, a step width of 0.0236° 2θ, a time per step of 0.54 s and CuKα radiation. The diffractometer was equipped with a LynxEye detection system. The goniometer radius of the diffractometer used was 280 mm, the 2θ angular range of the linear position sensitive detector was 2.942°. A fixed divergence slit with an angle of 0.3° was used. Primary and secondary Soller slits were used with an angle of 2.5°. Rietveld refinement using TOPAS 7.0 (Bruker AXS) was applied. Peak shape was modelled by the fundamental parameters approach. A Chebychev background of 1st order and a 1/x background were used for refinement. The stacking fault approach was implemented into the TOPAS software. In order to account for the potential variance in the interlayer spacing and movement of layers, a brucite structure was chosen from the ICSD database (collection code 34401 [23]) and adjusted. The sites and lattice parameters of the starting model are shown in Table S1 of the ESM. The structure was reduced to one layer consisting of one Mg and two oxygen sites and defined as layer A. In order to avoid any problems applying the stacking faults approach the symmetry was removed by creating a structure with the space group P1. The original c direction was then defined as the stacking direction. In the present study a number of 30 stacks was defined, and a movement of the stacks along x, y and z direction was allowed and refined during Rietveld refinement. Rotation of the layers against each other was not considered for the present study. Fig. 2 shows the adjusted structure of brucite with the defined layer A, the stacking direction and the movement plane where displacement of the layers against each other is refined in x, y and z direction. For hydromagnesite the structure with ICSD collection code 1591139 [24] was used. Atomic positions, thermal parameters and bond lengths were not refined for all phases.

For the fitting of the brucite in the samples cured at 60 °C a proper Rietveld refinement was only achievable after considering anisotropic domain size morphology. To this end a Topas macro considering anisotropic crystallites was applied. A cylindrical model for the crystallite size showed best results. For a deeper, theoretical background concerning anisotropic domain size morphology and its application in common Rietveld software the authors would like to refer to recent relevant literature [25,26].

4. Results

4.1. Summary of previous findings

In a previous study the compositions of the solid and the liquid phase of various mixtures between MgO and hydromagnesite were characterized at temperatures between 7 °C and 60 °C [11]. The main findings relevant for the present paper are summarized as follows:

1. When MgO hydrates in the presence of hydromagnesite, a brucite with a low crystallinity forms, whose reflections are broadened compared to those of the analytical brucite (Fig. 3). Furthermore, the 001 reflection appears to be shifted to higher 2θ values, and an additional hump occurs at around 16.1–16.8° 2θ Cu Kα (d-value range = 5.5–5.3 Å) for the sample cured at 20 °C. Previously this hump was tentatively assigned to an unknown magnesium carbonate hydrate phase [7,8]. In the sample cured at 60 °C this hump is no longer present, and the 001 reflection of brucite is at a very similar position than for the analytical grade brucite.
2. The mass losses in the TGA-IR of the sample cured at 20 °C (Fig. 4a) can be assigned mainly to brucite and hydromagnesite. The main decomposition peak of brucite at around 400 °C is overlapping with the 2nd decomposition peak of hydromagnesite related to loss of H_2O and CO_2. Thus, not only water, but also CO_2 is released at this temperature. According to mass balance calculations and also evident from previous investigations of a 90/10 blend [11], this CO_2-release cannot be assigned to the decomposition of hydromagnesite alone and thus must include the CO_2 loss of an unknown carbonate-containing phase. In the 60 °C sample this decomposition peak is still present (Fig. 4b), but mainly related to the decomposition of hydromagnesite. Furthermore, a mass loss is observed for the 20 °C sample at 30–160 °C, tentatively assigned to the presence of "gel" water. For the sample cured at 60 °C this mass loss is not very evident.

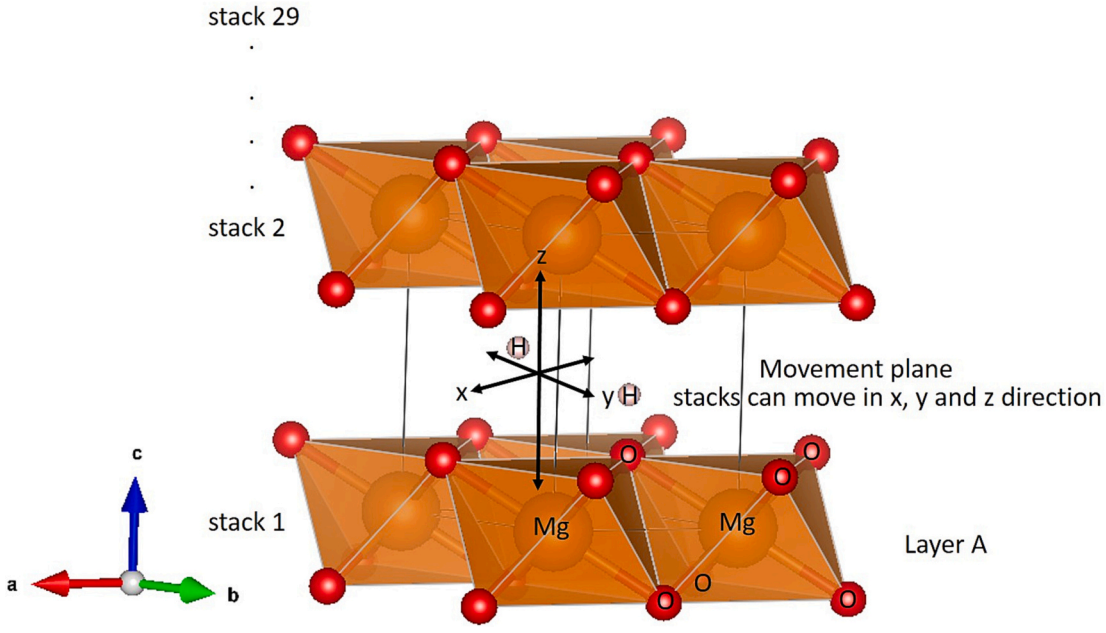

Fig. 2. Visualization of stacking layers in the brucite structure as well as movement plane and moving directions for stacking faults between repeating layer A (Visualization done using VESTA 3 [20]).

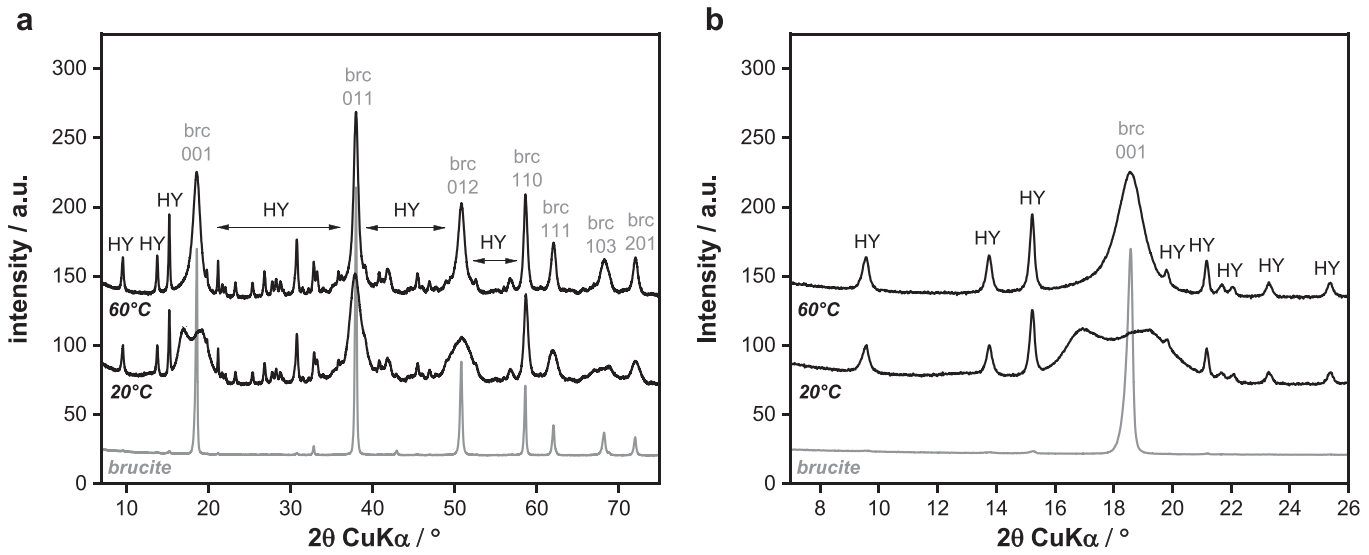

Fig. 3. XRD patterns of the 70/30 paste hydrated at 20 °C and 60 °C for 12 months. (a) Whole pattern, (b) detail of the pattern between 7 and 26° 2θ Cu Kα. Reagent-grade brucite as reference. brc = brucite, HY = hydromagnesite.

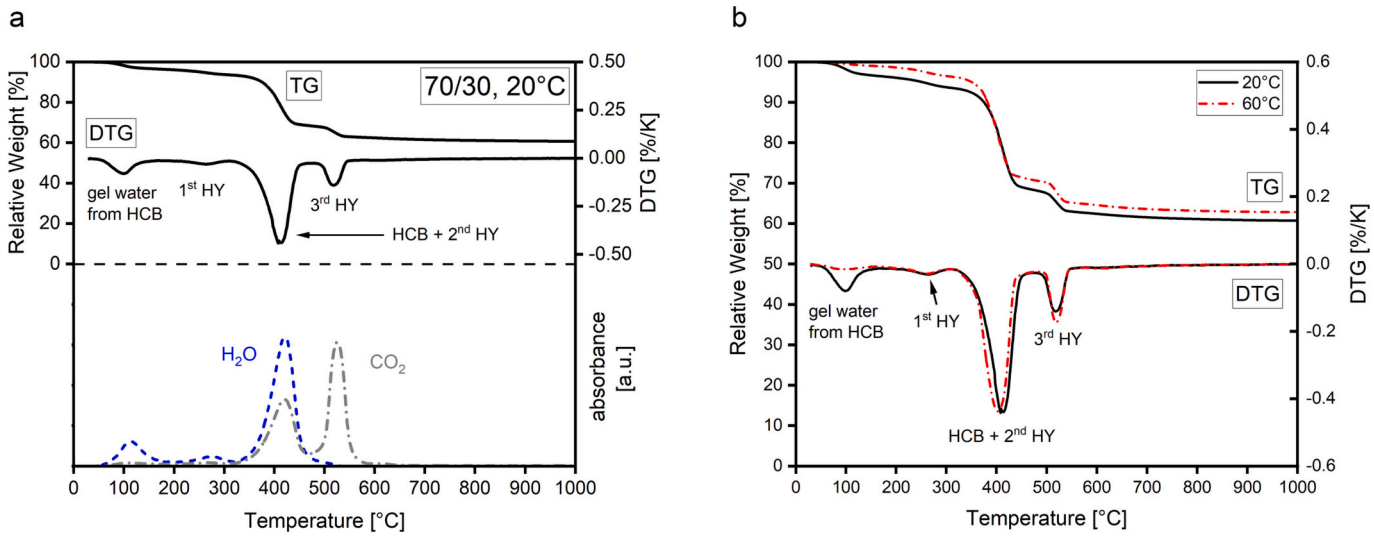

Fig. 4. (a) TGA/FTIR data of 70/30 paste hydrated at 20 °C for 12 months. Mass loss (TG) and differential mass loss (DTG) curves are displayed in the upper half of the diagram. IR signals of H_2O and CO_2 obtained from exhaust gas analysis by FTIR is shown below; (b) TGA/DTG data of 70/30 pastes hydrated at 20 and 60 °C for 12 months. Original data published in [11].

3. ^{13}C CP-MAS NMR of the sample cured at 20 °C (Fig. 5a) shows the presence of a signal at 173.0 ppm, which could not be assigned to any known magnesium carbonate phase. This signal is still present in the sample cured at 60 °C (Fig. 5b), however with a slightly lower intensity.
4. It was concluded from the results presented in [11] that no separate hydrated carbonate phase was present unlike previously suggested by [7,8]. Instead, the presence of a hydrous carbonate-containing brucite (HCB) of low crystallinity and with an approximate composition of $MgCO_3 \cdot 35\ Mg(OH)_2 \cdot H_2O$ based on mass balance calculations was postulated, and the thermodynamic data of this hypothetical phase were estimated. The additional hump present at around 16.1–16.8° 2θ Cu Kα in the XRD pattern of the sample cured at 20 °C was tentatively attributed to the HCB phase as well, probably related to the stacking sequence of the hydroxide sheets in the brucite structure.

4.2. Rietveld refinement of X-ray diffraction data of hydrated MgO/hydromagnesite blends

In all XRD patterns measured and evaluated in the present study only the crystalline phases HCB (hydrous carbonate-containing brucite) and hydromagnesite could be detected and were consequently used for the fitting of the XRD patterns. In Figs. 6 and 7 the reflections of the HCB phase are highlighted. All other reflections can be assigned to hydromagnesite.

Fig. 6 shows the Rietveld refinement of the MgO/hydromagnesite blend hydrated at 20 °C for 12 months. In Fig. 6a no stacking faults were considered. The two distinct reflections between 15 and 20° 2θ Cu Kα cannot be addressed by the use of the brucite structure [23] used as starting point in the refinement. The refinement of the brucite-like HCB-phase in the sample is thus very unsatisfying leading to a very poor difference plot. In Fig. 6b the movement of the stacks of layer A (Fig. 2) in the directions x and y are allowed. This leads to a better description of the structure of the brucite-like HCB-phase in the sample than in the

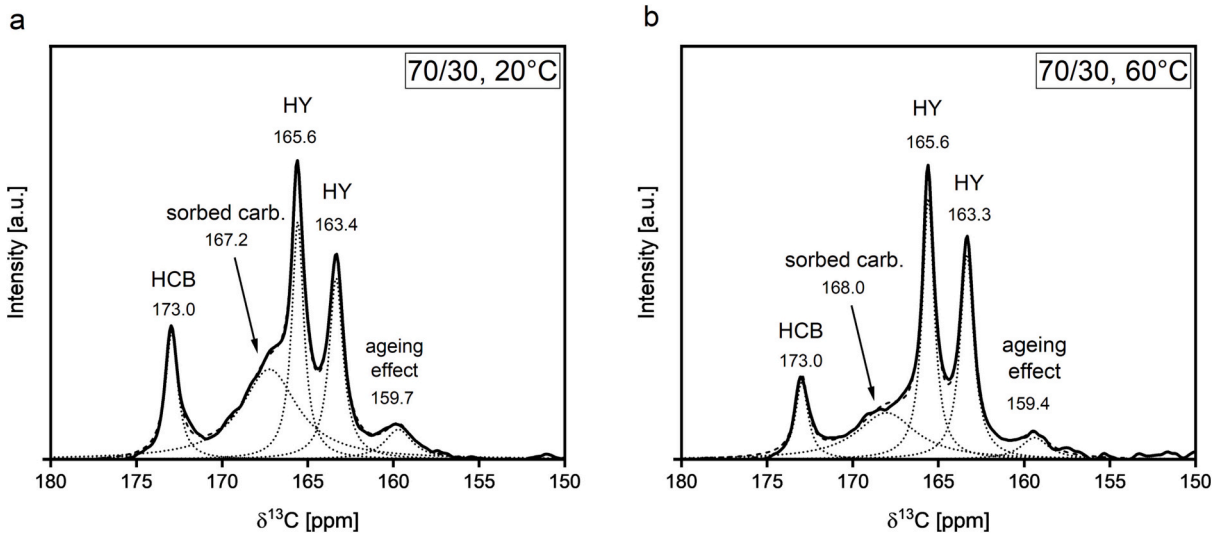

Fig. 5. ^{13}C CP-MAS NMR spectra with simulated shapes of individual resonances of 70/30 pastes cured at (a) 20 °C and (b) 60 °C for 12 months. The resonances at 163.4 ppm and 165.6 ppm are due to the presence of hydromagnesite [27,28], and the resonance at 167.0–168.0 ppm is tentatively assigned to the presence of sorbed CO_3^{2-}/HCO_3^- [29,30]. The resonances at 159.4–159.7 ppm and 173.0 ppm are tentatively assigned to carboxylic resonances A (probably an ageing effect of the samples as discussed in [11]) and B, respectively. Original data published in [11].

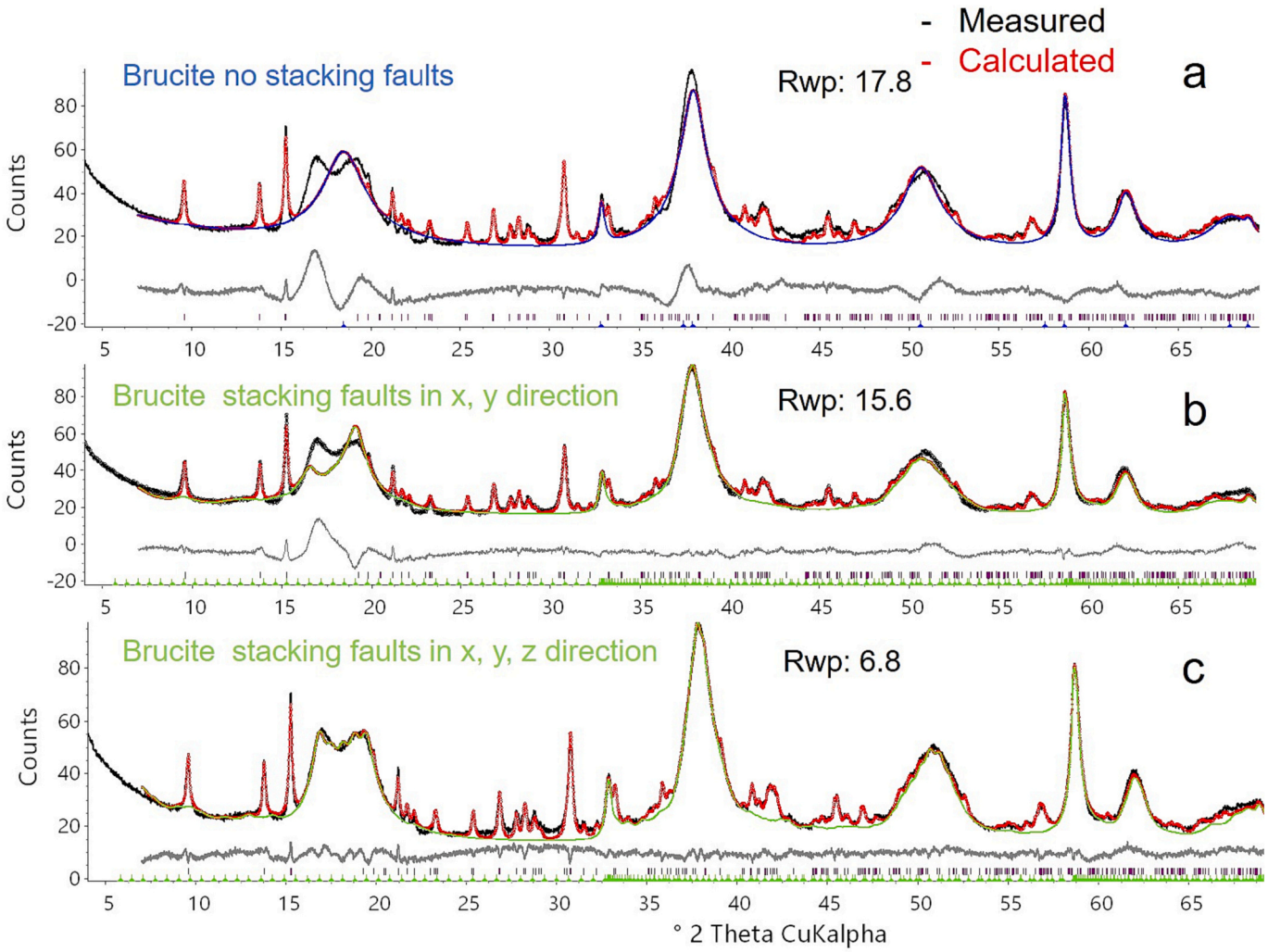

Fig. 6. Rietveld refinements of the XRD pattern of sample MgO/hydromagnesite 70/30 cured at 20 °C a) without stacking faults, b) considering stacking faults in x and y direction, and c) considering stacking faults in x, y and z direction. Rwp = weighted profile R-factor. All reflections, which are not assigned to the HCB phase (hydrous carbonate-containing brucite with stacking faults), can be assigned to the phase hydromagnesite.

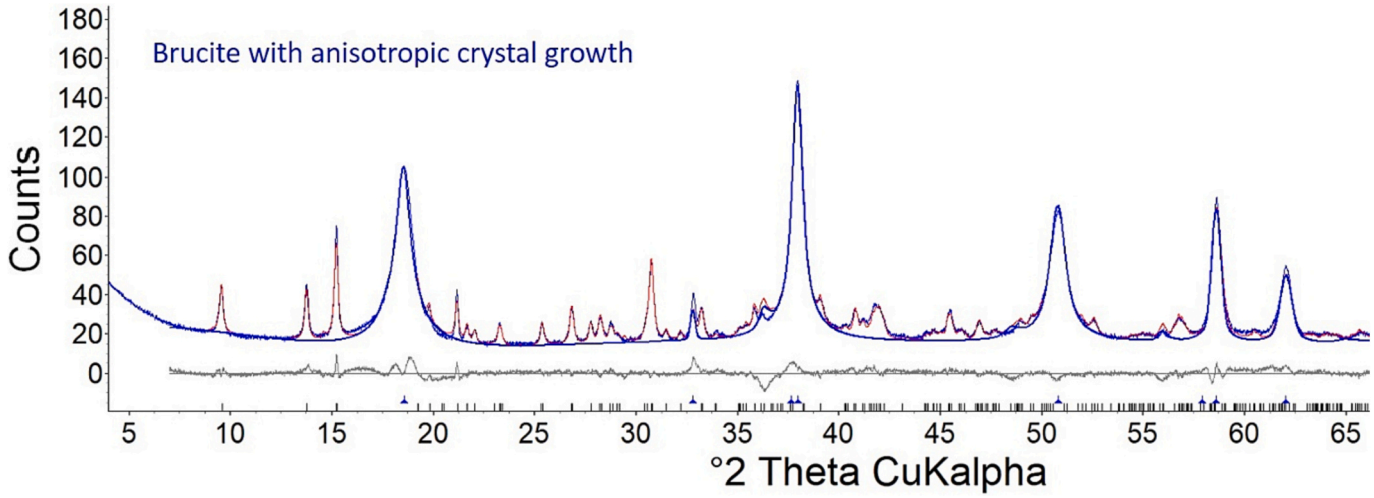

Fig. 7. Rietveld refinement of the XRD pattern of the sample MgO/hydromagnesite 70/30 cured at 60 °C with consideration of anisotropic crystal growth (Rwp: 11.2). All reflections, which are not assigned to the brucite with anisotropic crystal growth, can be assigned to the phase hydromagnesite.

previous case.

Finally, the refinement of the movement of the stacks in x, y and additionally also in z direction leads to a very accurate description of the recorded XRD pattern as it can be seen in Fig. 6c. Thus, it can be concluded that the brucite-like structure of the HCB-phase formed in the sample cured at 20 °C can be described very accurately with the stacking faults approach by allowing the stacks to move against each other in three directions in space (x, y, z). The hypothesis, that only one hydrate phase is present besides unreacted hydromagnesite [11] and not two as suggested earlier [7,8], could be confirmed.

In contrast to the sample cured at 20 °C, the sample cured at 60 °C does not show stacking faults as described above. The two distinct reflections between 15 and 20° 2θ Cu Kα are not visible in the sample stored at 60 °C. Only one reflection can be recorded as it can be assumed from the structure of brucite without stacking faults (Fig. 7). It has to be mentioned here that the brucite-like HCB-phase in the sample cured at 60 °C shows anisotropic peak broadening which has to be considered for a proper Rietveld refinement. Details about anisotropic peak broadening due anisotropic domain size morphology can be found elsewhere [25,26].

Table 1 provides the quantification of the residual hydromagnesite in the two samples determined by TGA, ^{13}C CP-MAS NMR and the newly performed Rietveld refinements of the XRD patterns. The results show that (i) all methods provide very comparable results, and (ii) that approximately 25–35 mass-% of the hydromagnesite present in the blend has reacted. The latter information was used in [11] to calculate the composition of the HCB-phase to be approximately $MgCO_3$·35 Mg$(OH)_2$·H_2O.

The refinement of the anisotropic brucite-like structure (HCB) in the 60 °C sample leads to lattice parameters of a = 3.148 Å and c = 4.774 Å. These values are very comparable to the starting brucite structure with a = 3.142 Å and c = 4.766 Å.

The refinement of the 20 °C sample leads to a lattice parameter a = 3.146 Å which indicates that the HCB structure (hydrous carbonate-containing brucite with stacking faults) is structurally comparable to the brucite structure. The lattice parameter c in a structure with stacking faults can be seen as an average parameter of all d-values in c-direction. In the brucite structure it is the average distance between 2 Mg sites in c-direction. The values for c of the refined structure containing stacking faults are between 4.67 Å and 5.26 Å, which corresponds to positions of the 001 reflection between 16.8 and 19.0° 2θ as it can be seen in the XRD patterns of the 20 °C sample. The refined distances between all the chosen 30 stacking layers are all between these two values.

Table 1
Amount of unreacted hydromagnesite in hydrated MgO/hydromagnesite pastes (70/30 by mass) calculated by TGA, ^{13}C CP-MAS NMR, and Rietveld refinement. TGA and ^{13}C NMR data previously published in [11].

Temperature	Hydromagnesite content [mass-%]		
	TGA	^{13}C CP-MAS NMR	Rietveld refinement
20 °C	18.4	16.2	16
60 °C	18.9	16.5	19

5. Conclusions

It could be shown that the brucite-like HCB-phase in the sample MgO/hydromagnesite 70/30 cured at 20 °C can be described by a brucite-like structure with stacking faults. It is postulated that the brucite-like structure of the HCB-phase has an average composition of $MgCO_3$·35 Mg$(OH)_2$·H_2O [11] resulting in the assumption that between the brucite layers certain amounts of H_2O and CO_2 can be incorporated, which in turn can give the decisive reason why the layers in the structure can be displaced against each other randomly in three directions in space. Fig. 8 shows a schematic illustration how the authors imagine the brucite-like structure in the 20 °C sample.

The sample cured at 60 °C does not contain significant amounts of "gel water" as shown by TGA (Fig. 4), and the content of carbonate seems to be lower than for the sample cured at 20 °C as derived from ^{13}C CP-MAS NMR. Thus, it can be hypothesized that at 60 °C the brucite-like phase is still poorly ordered, but consists of brucite layers with similar d-spacing of the 001 reflection incorporating only (hydrogen)carbonate between the layers.

However, although it could be shown that carbonate is incorporated in the structure, further considerations are needed to achieve a deeper understanding how the incorporation of carbonate can be explained. At a measured pH value of approximately 10–11 [11], the aquatic speciation is dominated by HCO_3^- and CO_3^{2-}, while only minor amounts of H_2CO_3 are present. Thus, it has to be discussed how the charge balance in a HCB structure can be maintained if charged species such as HCO_3^- and CO_3^{2-} are incorporated into the structure. Either, H_2CO_3 is incorporated, and the very low amount of dissolved H_2CO_3 at a pH value in the order of 10–11 is the reason why only very low amounts are incorporated in the HCB structure. Alternatively, if the charged species HCO_3^- and CO_3^{2-} are incorporated, it seems probable that some OH^- sites are occupied by e.g. HCO_3^- in the structure. Fig. 8 shows the incorporation of HCO_3^- as a possible example. The presented data cannot clarify this issue as the refinement of stacking faults combined with a structure

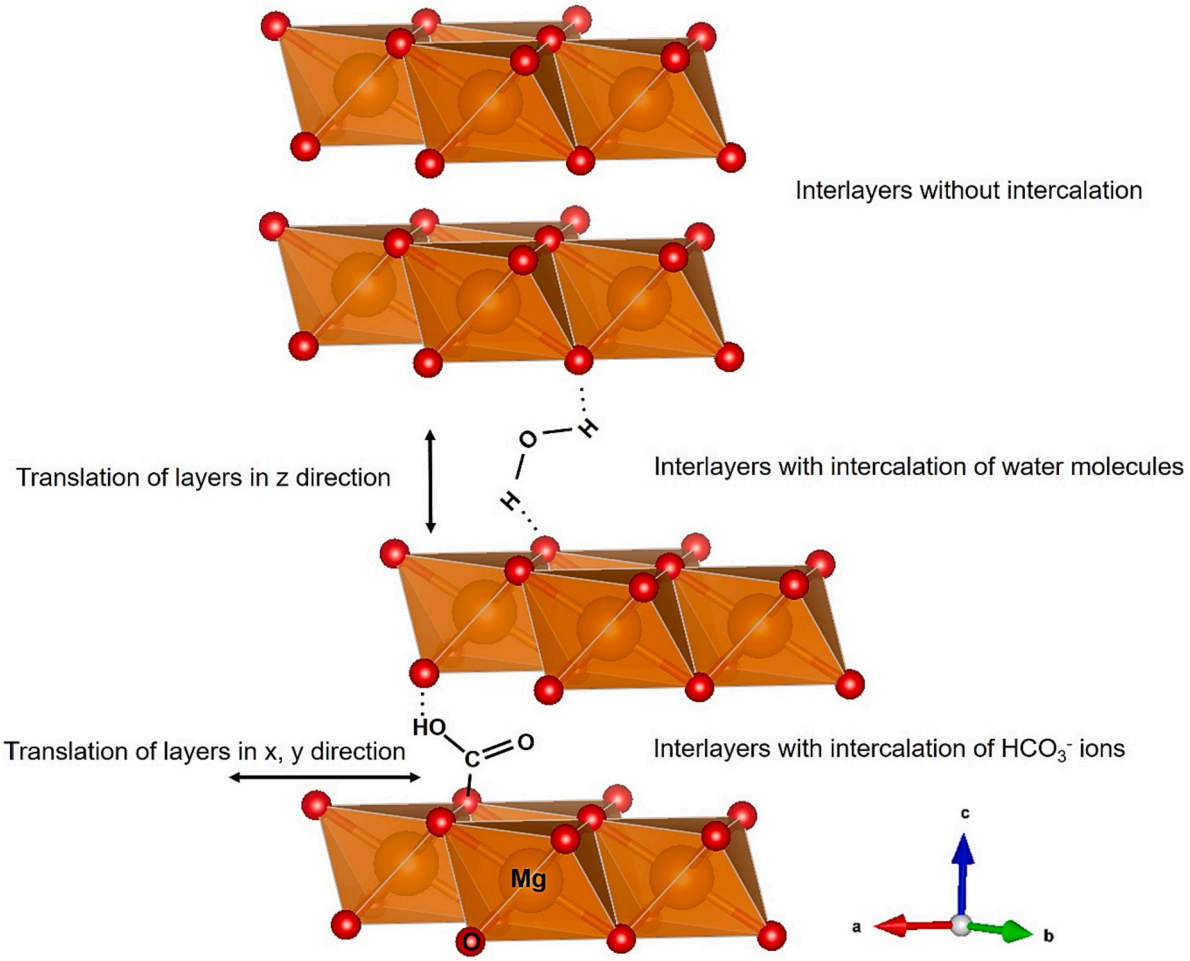

Fig. 8. Visualization of the possible brucite-like structure using VESTA 3 [20]. The possible intercalation options are shown in the figure. The sequence of the interlayers is shown as an example. The sequence in the real structure is probably an arbitrary combination of the possible interlayers.

refinement and/or solution using the available XRD data would be too imprecise. Most challenging is the low crystallinity of the HCB phase as visible by the broad reflections in the XRD patterns.

CRediT authorship contribution statement

Daniel Jansen: Conceptualization, Methodology, Investigation, Writing – original draft. **Alexander German:** Conceptualization, Methodology, Investigation, Writing – original draft. **Dominique Ectors:** Methodology, Writing – review & editing. **Frank Winnefeld:** Conceptualization, Writing – original draft.

Declaration of competing interest

The authors declare that they have no known competing financial interests or personal relationships that could have appeared to influence the work reported in this paper.

Data availability

Data will be made available on request.

Acknowledgements

Barbara Lothenbach, Pietro Lura, Daniel Rentsch (Empa) and Jürgen Neubauer (FAU) are acknowledged for fruitful discussions.

Appendix A. Supplementary data

Supplementary data to this article can be found online at https://doi.org/10.1016/j.cemconres.2023.107371.

References

[1] E. Gartner, T. Sui, Alternative cement clinkers, Cem. Concr. Res. 114 (2018) 27–39.
[2] E. Bernard, H. Nguyen, S. Kawashima, B. Lothenbach, H. Manzano, J.L. Provis, A. Scott, C. Unluer, F. Winnefeld, P. Kinnunen, MgO-based cements – current status and opportunities, RILEM Tech. Lett., accepted.
[3] N. Vlasopoulos, Waste Minimisation through Sustainable Magnesium Oxide Cement Products, PhD Thesis, Imperial College, London, UK, 2007.
[4] N. Vlasopoulos, C.R. Cheeseman, Binder Composition, PCT Patent Application PCT/GB2009/001610,, International Publication Number WO, 12/30/2009, 2009/156740 A1.
[5] F. Zhang, Magnesium Oxide Based Binders as Low-Carbon Cements, PhD Thesis, Imperial College, London, UK, 2012.
[6] F. Winnefeld, A. Leemann, A. German, B. Lothenbach, CO_2 storage in cement and concrete by mineral carbonation, Curr. Opin. Green Sustain. Chem. 38 (2022), 100672.
[7] C. Kuenzel, F. Zhang, V. Ferrándiz-Mas, C.R. Cheeseman, E.M. Gartner, The mechanism of hydration of MgO-hydromagnesite blends, Cem. Concr. Res. 103 (2018) 123–129.
[8] F. Winnefeld, E. Epifania, F. Montagnaro, E.M. Gartner, Further studies of the hydration of MgO-hydromagnesite blends, Cem. Concr. Res. 126 (2019), 105912.
[9] H.C. Helgeson, J.M. Delany, H.W. Nesbitt, D.K. Bird, Summary and critique of the thermodynamic properties of rock-forming minerals, Am. J. Sci. 278A (1978) 1–229.
[10] J.W. Johnson, E.H. Oelkers, H.C. Helgeson, SUPCRT92 - a software package for calculating the standard molal thermodynamic properties of minerals, gases, aqueous species, and reactions from 1 to 5000 bar and 0 1000°C, Comput. Geosci. 18 (1992) 899–947.

[11] A. German, F. Winnefeld, P. Lura, D. Rentsch, B. Lothenbach, Hydrous carbonate-containing brucite (HCB) in MgO/hydromagnesite blends, Cem. Concr. Res. 173 (2023), 107304.
[12] A. German, Potential Use of a Low-Carbon Magnesia (MgO) Binder for Construction Purposes, PhD Thesis, ETH Zürich, Switzerland, 2024.
[13] K. Lawson, S.P. Wallbridge, A.E. Catling, C.A. Kirk, S.E. Dann, Determination of layered nickel hydroxide phases in materials disordered by stacking faults and inter-stratification, J. Mater. Chem. A 11 (2023) 789–799.
[14] A.A. Coelho, J.S.O. Evans, J.W. Lewis, Averaging the intensity of many-layered structures for accurate stacking-fault analysis using Rietveld refinement, J. Appl. Cryst. 49 (2016) 1740–1749.
[15] K. Ufer, G. Roth, R. Kleeberg, H. Stanjek, R. Dohrmann, J. Bergmann, Description of X-ray powder pattern of turbostratically disordered layer structures with a Rietveld compatible approach, Z. Krist. – Cryst. Mater. 219 (2004) 519–527.
[16] K. Ufer, R. Kleeberg, T. Monecke, Quantification of stacking disordered Si–Al layer silicates by the Rietveld method: application to exploration for high-sulphidation epithermal gold deposits, Powd. Diffr. 30 (2015) S111–S118.
[17] B.A. Sakharov, V.A. Drits, D.K. McCarty, G.M. Walker, Modeling powder X-ray diffraction patterns of the clay minerals society kaolinite standards: KGa-1, KGa-1b, and KGa-2, Clays Clay Mineral. 64 (2016) 314–333.
[18] X. Wang, R.D. Hart, J. Li, R.G. McDonald, A. van Riessen, Quantitative analysis of turbostratically disordered nontronite with a supercell model calibrated by the PONKCS method, J. Appl. Cryst. 45 (2012) 1295–1302.
[19] X. Wang, J. Li, R.D. Hart, A. van Riessen, R. McDonald, Quantitative X-ray diffraction phase analysis of poorly ordered nontronite clay in nickel laterites, J. Appl. Cryst. 44 (2011) 902–910.
[20] K. Momma, F. Izumi, VESTA 3 for three-dimensional visualization of crystal, volumetric and morphology data, J. Appl. Cryst. 44 (2011) 1272–1276.
[21] R. Snellings, J. Chwast, Ö. Cizer, N. De Belie, Y. Dhandapani, P. Durdzinski, J. Elsen, J. Haufe, D. Hooton, C. Patapy, M. Santhanam, K. Scrivener, D. Snoeck, L. Steger, T. Sui, A. Vollpracht, F. Winnefeld, B. Lothenbach, RILEM TC-238 SCM recommendation on hydration stoppage by solvent exchange for the study of hydrate assemblages, Mater. Struct. 51 (2018) 172.
[22] D. Massiot, F. Fayon, M. Capron, I. King, S. Le Calvé, B. Alonso, J.-O. Durand, B. Bujoli, Z. Gan, G. Hoatson, Modelling one- and two-dimensional solid-state NMR spectra, Magnet. Reson. Chem. 40 (2002) 70–76.
[23] F. Zigan, R. Rothbauer, Neutronenbeugungsmessungen am Brucit, N. Jahrb. Mineral., Monatsh. (1967) 137–143.
[24] M. Akao, S. Iwai, The hydrogen bonding of hydromagnesite, Acta Cryst. B 33 (1977) 1273–1275.
[25] D. Ectors, F. Götz-Neunhoeffer, J. Neubauer, A generalized geometric approach to anisotropic peak broadening due to domain morphology, J. Appl. Cryst. 48 (2015) 189–194.
[26] D. Ectors, F. Götz-Neunhoeffer, J. Neubauer, Domain size anisotropy in the double-Voigt approach: an extended model, J. Appl. Cryst. 48 (2015) 1998–2001.
[27] J.K. Moore, J.A. Surface, A. Brenner, L.S. Wang, P. Skemer, M.S. Conradi, S. E. Hayes, Quantitative identification of metastable magnesium carbonate minerals by solid-state ^{13}C NMR spectroscopy, Environm, Sci. Technol. 49 (2015) 1986.
[28] J.L. Cui, D.L. Olmsted, A.K. Mehta, M. Asta, S.E. Hayes, NMR crystallography: evaluation of hydrogen positions in hydromagnesite by ^{13}C {^{1}H} REDOR solid-state NMR and density functional theory calculation of chemical shielding tensors, Angew. Chem. Int. Edit. 58 (2019) 4210–4216.
[29] S. Ishihara, P. Sahoo, K. Deguchi, S. Ohki, M. Tansho, T. Shimizu, J. Labuta, J. P. Hill, K. Ariga, K. Watanabe, Y. Yamauchi, S. Suehara, N. Iyi, Dynamic breathing of CO_2 by hydrotalcite, J. Am. Chem. Soc. 135 (2013) 18040–18043.
[30] E. Bernard, B. Lothenbach, D. Rentsch, A. German, F. Winnefeld, Effect of carbonates on the formation of magnesium silicate hydrates, Mater. Struct. 55 (2022) 183.